

Advantage of quantum coherence in postselected metrology

Shao-Jie Xiong,^{1,2} Peng-Fei Wei,¹ Huang-Qiu-Chen Wang,¹ Lei Shao,²
Yong-Nan Sun,¹ Jing Liu,^{3,*} Zhe Sun,^{1,†} and Xiao-Guang Wang^{2,‡}

¹*School of physics, Hangzhou Normal University, Hangzhou 310036, China*

²*Zhejiang Institute of Modern Physics and Department of Physics,
Zhejiang University, Hangzhou, Zhejiang 310027, China*

³*National Precise Gravity Measurement Facility, MOE Key Laboratory of Fundamental Physical Quantities Measurement,
School of Physics, Huazhong University of Science and Technology, Wuhan 430074, China*

In conventional measurement, to reach the greatest accuracy of parameter estimation, all samples must be measured since each independent sample contains the same quantum Fisher information. In postselected metrology, postselection can concentrate the quantum Fisher information of the initial samples into a tiny post-selected sub-ensemble. It has been proven that this quantum advantage can not be realized in any classically commuting theory. In this work, we present that the advantage of postselection in weak value amplification (WVA) can not be achieved without quantum coherence. The quantum coherence of the initial system is closely related to the preparation costs and measurement costs in parameter estimation. With the increase of initial quantum coherence, the joint values of preparation costs and measurement costs can be optimized to smaller. Moreover, we derive an analytical tradeoff relation between the preparation, measurement and the quantum coherence. We further experimentally test the tradeoff relation in a linear optical setup. The experimental and theoretical results are in good agreement and show that the quantum coherence plays a key role in bounding the resource costs in the postselected metrology process.

Parameter estimation is a fundamental subject in information theory and mathematical statistics. In quantum metrology, the precision can be improved beyond classical bounds by quantum effect, and the lower-bounds of variance is determined by the quantum Cramér-Rao inequality [1–4],

$$\langle (g - g_{\text{est}})^2 \rangle \geq \frac{1}{\nu F}, \quad (1)$$

where g is the parameter to be estimated, g_{est} is an unbiased estimator for g , ν is the number of independent samples, and F is the quantum Fisher information (QFI) for a single sample. The quantum Cramér-Rao bound describes the theoretical precision limit in parameter estimation. However, a realistic parameter estimation process must take into account many factors, such as the limitation in preparation of samples, the technical noise of detectors [5], and the impact of decoherence [6]. Moreover, multiparameter estimation has to be considered in some cases [7–9].

Weak-value amplification (WVA) is a metrological protocol to amplify ultrasmall physical effects by postselection, and has some obvious advantages over conventional measurement under the influence of environmental noises [10–14]. It has been widely used for precision measurements of weak signals, such as the spin Hall effect of light [15], phase shifts [16, 17], frequency shifts [18], tiny deflections of light [19], and velocity measurements [20]. Under the Fisher information metric [21–25], WVA can put all of the Fisher information of initial samples into a small number of post selected samples. It implies that WVA can overcome the technical noise caused by the low saturation of detectors. This advantage has been experimentally demonstrated in optical systems [26]. In

Ref. [23], the authors prove that the advantage of postselection can only be realized in nonclassical metrology.

In parameter estimation experiments, the preparation and measurement of quantum states require a certain cost. For example, the preparation costs can be the time or energy needed to prepare the samples, and the measurement costs can be the time or energy needed to reset the detector after a detection. It is important to investigate how to reduce these costs and thus obtain the higher accuracy of parameter estimation.

In this work, we focus on the problem about the preparation costs and measurement costs in the parameter estimation by WVA. The effect of WVA is determined by the pre-and post-selection states. For a general initial state, it is found that the two costs cannot always reach the minimum jointly in the WVA scenario. We derive a trade-off relation between the two costs and reveal that the two costs are constrained by the quantum coherence in the initial system state. Concretely, if and only if the initial state of system is prepared in the maximum coherent states, the two costs can be taken to the minimum value jointly, i.e., WVA performs the best advantage. While for the incoherent states, the two costs are impossibly smaller than the case in conventional measurement, which implies WVA has no any advantages. Consequently, quantum coherence is an indispensable resource to realize the technical advantage of WVA. More importantly, we give an analytical tradeoff relation between the two costs and the quantum coherence. Our theory is expected to have useful applications in the parameter-estimation experiments, where the consumption during the preparation and measurement process should be treated differently. Finally, we experimen-

tally test the effect of quantum coherence on the tradeoff of the two costs in linear optical systems.

We consider that the estimation of the parameter g is introduced by the unitary evolution

$$U(g) = \exp(-igA \otimes M), \quad (2)$$

where M and A are the operators of meter (denoted by m) and system (denoted by s) respectively, $|\Psi_i\rangle = |\psi_{si}\rangle|\phi_{mi}\rangle$ is the separable initial state, and g is the coupling strength and also the parameter to be estimated. The QFI of g is defined by

$$F = 4(|\partial_g \langle \Psi(g) | | \partial_g | \Psi(g) \rangle| - |\partial_g \langle \Psi(g) | | \Psi(g) \rangle|^2) \quad (3)$$

where $|\Psi(g)\rangle = U(g)|\Psi_i\rangle$. According to the above expression, we can easily get the QFI of g

$$F = 4(\langle A^2 \rangle \langle M^2 \rangle - \langle A \rangle^2 \langle M \rangle^2). \quad (4)$$

We assume that the initial state of meter is at the balance zero point, i.e., $\langle M \rangle = 0$, and the average of M^2 in the initial state is defined by $\Omega \equiv \langle M^2 \rangle$. Under these conditions, we have $F = 4\langle A^2 \rangle \Omega$.

Parameter estimation under conventional measurement. To begin with, we identify $[NF]^{-1}$ as the metric of the estimation accuracy, where N is the number of the samples and here it is assumed to be large enough. Under conventional measurement, $R_p N$ is defined as the minimum preparation costs to finish the parameter estimation task, where R_p is the cost to prepare one sample. $R_m N$ is the corresponding minimum measurement costs to detect all samples, where R_m is the cost to detect one sample.

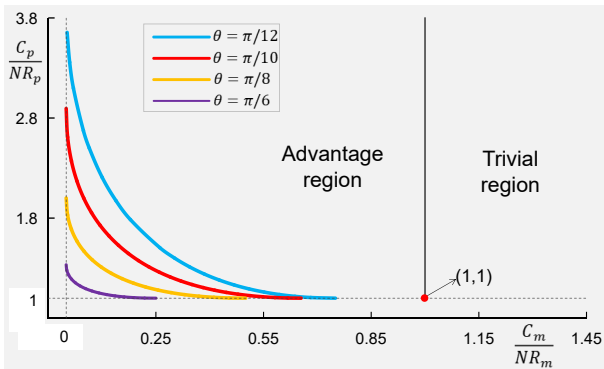


Figure 1. Preparation costs and measurement costs for the initial state $|\psi_i\rangle_s = \cos(\theta)|\hat{0}\rangle + \sin(\theta)|\hat{1}\rangle$. The regions below the curves are forbidden.

Parameter estimation under WVA protocol. Consider the unitary evolution in Eq. (2), the probability to detect the system in the post-selection state $|\psi_{sf}\rangle$ is $p = |\langle \psi_{sf} | U(g) | \psi_{si} \rangle \langle \phi_{mi} | |^2$, and the corresponding collapsed state of meter is

$$|\phi_{mf}(g)\rangle = \langle \psi_{sf} | U(g) | \psi_{si} \rangle |\phi_{mi}\rangle / \sqrt{p}. \quad (5)$$

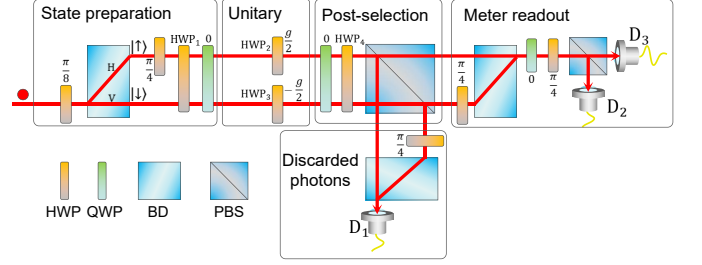


Figure 2. Experimental implementation to estimate a polarization change via WVA. The angles of all QWPs are set to 0. The devices are half-wave plates (HWP), quarter-wave plates (QWP), beam displacers (BD) and polarizing beam splitters (PBS).

When g is sufficiently small, the QFI of g in the collapsed state $|\phi_{mf}(g)\rangle$ is

$$F_m(g) = 4\Omega |A_w|^2 + \mathcal{O}_F(g), \quad (6)$$

where $A_w = \langle \psi_{sf} | A | \psi_{si} \rangle / \langle \psi_{sf} | \psi_{si} \rangle$ is the weak value [22], $\mathcal{O}_F(g)$ is the high-order terms of g in the expression of the QFI F_m . The postselection success probability is $p = |\langle \psi_{sf} | \psi_{si} \rangle|^2 + \mathcal{O}_p(g)$, where $\mathcal{O}_p(g)$ is the high-order terms of g in the expression of the probability p . The probabilistic QFI is

$$f_m = p \cdot F_m = 4\Delta |\langle \psi_{sf} | A | \psi_{si} \rangle|^2 + \mathcal{O}(g). \quad (7)$$

where $\mathcal{O}(g)$ denotes the high-order terms of g which is with respect to $\mathcal{O}_F(g)$ and $\mathcal{O}_p(g)$. In WVA, preparation costs and measurement costs are denoted by C_p and C_m respectively, and the number of samples needed in the WVA is denoted by n . To achieve the accuracy target $(NF)^{-1}$, n should be satisfied $nf_m = NF$, then we can get $C_p = nR_p = \frac{F}{f_m} R_p N$. The number of postselection samples is np and the corresponding measurement costs is $C_m = npR_m$. At last, we have

$$C_p = \frac{F}{f_m} R_p N, \quad C_m = \frac{F}{F_m} R_m N. \quad (8)$$

We first analyze the effect of the postselection state $|\psi_{sf}\rangle$ on C_p and C_m . The optimal state $|\psi_{sf}^{\text{opt}}\rangle$, which is defined as $|\psi_{sf}^{\text{opt}}\rangle = A|\psi_{si}\rangle / \sqrt{\langle A^2 \rangle}$ [22], can make $f_m(|\psi_{sf}^{\text{opt}}\rangle)$ take the maximum, which can approximately equal to F , but cannot be larger than it [22]. Then, the minimum value of C_p satisfies $C_p(|\psi_{sf}^{\text{opt}}\rangle) \gtrsim R_p N$, but the measurement costs $C_m(|\psi_{sf}^{\text{opt}}\rangle)$ may not achieve the minimum. The near-orthogonal state $|\psi_{sf}^{\perp}\rangle$, which is defined as $\langle \psi_{si} | \psi_{sf}^{\perp} \rangle \approx 0$, can make $C_m(|\psi_{sf}^{\perp}\rangle)$ take the minimum value since the weak value A_w in Eq. (6) can approach its maximum at the near-orthogonal state $|\psi_{sf}^{\perp}\rangle$. However, the preparation costs $C_p(|\psi_{sf}^{\perp}\rangle)$ cannot reach its minimum.

To minimize C_p and C_m jointly, the initial state of system should be prepared in the special states. We consider

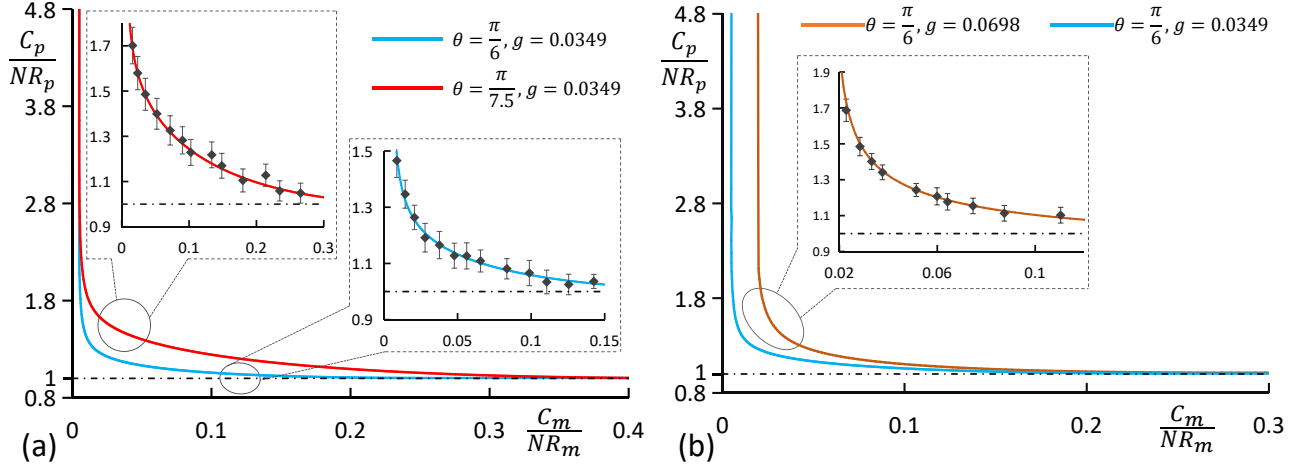


Figure 3. Experimental data of the tradeoff bound of C_p and C_m for the initial state $|\psi_{si}\rangle = \cos(\theta)|\tilde{0}\rangle + \sin(\theta)|\tilde{1}\rangle$. The experimental data are denoted by rhombuses. Solid lines correspond to theoretical results. (a) Different parameters to be estimated, i.e., $g = 0.0349$ rad and 0.0698 rad. The parameter $\theta = \pi/6$. In the experiment, $\sigma = \sigma_y$ with the eigenstates $|\tilde{0}\rangle = 1/\sqrt{2}(|H\rangle + i|V\rangle)$ and $|\tilde{1}\rangle = 1/\sqrt{2}(|H\rangle - i|V\rangle)$, $M = \sigma_z$ with the eigenstates $|\uparrow\rangle$ and $|\downarrow\rangle$.

that the system s is a qubit system and let $A = \sigma$ which is one of the Pauli operators, then $|\psi_{sf}^{\text{opt}}\rangle = \sigma|\psi_{si}\rangle$ and $F = 4\Omega$ since $\langle\sigma^2\rangle = 1$. We define the eigenstates of σ are $|\tilde{0}\rangle, |\tilde{1}\rangle$ with the eigenvalues 1 and -1 . For a general two-dimensional state, the density operator can be represented by $\rho = \frac{1}{2}(I + \mathbf{r} \cdot \boldsymbol{\sigma})$, where I is the 2×2 identity matrix, $\mathbf{r} = (r_1, r_2, r_3)$ is the Bloch vector, and $\boldsymbol{\sigma} = (\sigma_x, \sigma_y, \sigma_z)$ is the vector of Pauli matrices. For two pure states $|a\rangle$ and $|b\rangle$, the module square of the overlap $|\langle a|b\rangle|^2$ can be written as

$$|\langle a|b\rangle|^2 = \cos^2\left(\frac{1}{2}\Theta(\mathbf{r}_a, \mathbf{r}_b)\right), \quad (9)$$

where $\Theta(\mathbf{r}_a, \mathbf{r}_b) = \arccos(\mathbf{r}_a \cdot \mathbf{r}_b)$ is the angle between \mathbf{r}_a and \mathbf{r}_b . When the high-order of g in Eq. (8) can be neglected, C_p and C_m can be written as

$$\begin{aligned} C_p &= \frac{1}{\cos^2(\Theta(\mathbf{r}_1, \mathbf{r}_2)/2)} R_p N, \\ C_m &= \frac{C_p}{R_p} \cos^2(\Theta(\mathbf{r}_1, \mathbf{r}_3)/2) R_m, \end{aligned} \quad (10)$$

where $\mathbf{r}_1, \mathbf{r}_2, \mathbf{r}_3$ are Bloch vectors of $|\psi_{sf}\rangle, \sigma|\psi_{si}\rangle, |\psi_{si}\rangle$. The tradeoff relation of C_p and C_m can be obtained based on the geometric relationship $|\Theta(\mathbf{r}_1, \mathbf{r}_2) - \Theta(\mathbf{r}_1, \mathbf{r}_3)| \leq \Theta(\mathbf{r}_2, \mathbf{r}_3)$, then we have

$$\begin{aligned} &\left| 2 \arccos\left(\sqrt{\frac{R_p N}{C_p}}\right) - 2 \arccos\left(\sqrt{\frac{C_m R_p}{C_p R_m}}\right) \right| \\ &\leq 2 \arccos(\sqrt{1 - C_{l_1}(|\psi_{si}\rangle)}), \end{aligned} \quad (11)$$

where $C_{l_1}(|\psi_{si}\rangle)$ is the l_1 -norm of coherence of the initial state under the reference basis $\{|\tilde{0}\rangle, |\tilde{1}\rangle\}$. For a quantum state ρ , C_{l_1} can be calculated by $C_{l_1}(\rho) = \sum_{i \neq j} |\rho_{ij}|$,

where ρ_{ij} is the element of the density matrix in the space spanned by the reference bases $\{|\tilde{0}\rangle, |\tilde{1}\rangle\}$.

From Eq. (11), we find that the minimum value of C_m is restricted as $C_m = 1 - C_{l_1}^2$ when C_p takes the minimum value $C_p = NR_p$. Obviously, if and only if the initial state is the maximally coherent state, i.e., $C_{l_1} = 1$, the minimum values of C_p and C_m can be reached simultaneously. As shown in Fig.1, we demonstrate the bound on C_p and C_m for the initial states with different amounts of coherence resource. It should be noted that the condition of WAV should always be satisfied in Fig. 1, i.e., $g|A_w|\Omega \ll 1$, and the measurement costs C_m can not be zero in experiments. On the other hand, for any incoherent states, i.e., $\rho_{si} = \mu|\tilde{0}\rangle\langle\tilde{0}| + (1 - \mu)|\tilde{1}\rangle\langle\tilde{1}|$, we have $F = 4\Omega$ (see details in the Appendix). It can be proved that the QFI in the post-selection state cannot exceed F when the initial system state is incoherent, i.e., $F_m \leq F$ (the details are shown in the Appendix). It implies the measurement cost C_m is larger than that in the conventional scenario, i.e., $C_m \geq R_m N$. In this case, the WAV scenario cannot provide any advantages. Hence, we define the left side of $\frac{C_m}{NR_m} = 1$ as the advantage region while the right side as the trivial region.

Experimental setup. To demonstrate the effect of quantum coherence in the WVA scenario of parameter estimation, we experimentally estimate a tiny polarization angle change of a single photon. The experimental setup is sketched in Fig. 2. A single-photon source is produced via a spontaneous parametric down-conversion (SPDC) process by pumping a 1.5-cm-long type-II periodically poled potassium titanyl phosphate (PPKTP) nonlinear crystal with ultraviolet pulses at a 405 nm centered wavelength. One photon is directly detected as a trigger. The other one is prepared in a pure state of the spatial modes and

the polarization modes.

We employ the horizontal and vertical polarization modes $|H\rangle$ and $|V\rangle$ as the system basis vectors. And the spatial modes $|\uparrow\rangle$ and $|\downarrow\rangle$ act as the basis vectors of the meter. In the state preparation, the state $|\phi_{mi}\rangle = \frac{1}{\sqrt{2}}(|\uparrow\rangle + |\downarrow\rangle)$ of the meter is prepared by adjusting the first HWP to $\pi/8$. The state $|\psi_{si}\rangle = \cos(\theta)|\tilde{0}\rangle + \sin(\theta)|\tilde{1}\rangle$ of polarization can be prepared by adjusting the HWP₁ to $\pi/8 - \theta/2$, where $|\tilde{0}\rangle = 1/\sqrt{2}(|H\rangle + i|V\rangle)$ and $|\tilde{1}\rangle = 1/\sqrt{2}(|H\rangle - i|V\rangle)$. The unitary evolution is $U = \exp(ig\sigma_y^s \otimes \sigma_z^m)$, where $\sigma_y^s = i(|H\rangle\langle V| - |V\rangle\langle H|)$, $\sigma_z^m = |\uparrow\rangle\langle\uparrow| - |\downarrow\rangle\langle\downarrow|$, and the change of g is implemented by rotating the angles of HWP₂ and HWP₃ to $g/2$ in opposite directions. Then, the polarization mode is projected onto $|\psi_{sf}\rangle$ by postselecting the photon coming from the direct path of the PBS, and the post-selection state $|\psi_{sf}\rangle = \cos(\alpha)|\tilde{0}\rangle + \sin(\alpha)|\tilde{1}\rangle$ is determined by rotating HWP₄. To detect the probability of successful post-selection, the reflected discarded photons are measured by the D_1 detector. Finally, the meter readout is provided by the detectors D_2 and D_3 .

Experimental result. We demonstrate the cost ratios between conventional measurement and weak measurement with the initial system state $\cos(\theta)|\tilde{0}\rangle + \sin(\theta)|\tilde{1}\rangle$. According to Eq. (8), we experimentally represent $C_p/[NR_p]$ and $C_m/[NR_m]$ by detecting p and F_m . The Cramer-Rao bound is asymptotically attainable by the maximum likelihood estimator, thus the Fisher information is approximately obtained by measuring the variance of g_{est} , i.e., $F_m \simeq [\nu\delta^2 g_{\text{est}}]^{-1}$. We detect about 700 post-selection photons and collect the measurement outcomes from the two detectors D_2 and D_3 . Then the estimator g_{est} is obtained with the maximum likelihood, which maximizes the posterior probability based on the obtained data. The above process is repeated 1000 times to get the distribution and the variance of g_{est} .

In Fig. 3(a), the experimental and theoretical results are in good agreement and show the tradeoff bound between C_p and C_m for the superposition coefficients $\theta = \pi/6$ and $\theta = \pi/7.5$ with $g = 0.0349$ rad. The regions below the curves are forbidden. If $|\tilde{0}\rangle$ and $|\tilde{1}\rangle$ are defined as the reference bases, the l_1 -norm of coherence is $C_{l_1}(|\psi_{si}\rangle) = \sin(2\theta)$, and the more coherence resource of the initial state ($\theta \rightarrow \pi/4$) would give the lower cost. The curves in Fig. 3(a) is a little different from that in Fig. 1, where C_m can not be infinitely close to 0. This is because g is a finitely small parameter, and the regime of validity of the weak-value theory can not be satisfied when A_w is too large. In Fig. 3(b), we compare the tradeoff bound with $g = 0.0349$ rad and 0.0698 rad by setting $\theta = \pi/6$. The tradeoff bound provided by Eq. (11) becomes more tight when g is smaller.

Conclusion. In the actual parameter estimation process, it is necessary to consider the consumption of preparation resources and measurement resources. In this

work, we investigated the problem of the resource cost in the weak-value amplification. We derive a tradeoff relation between the preparation costs, measurement costs, and the quantum coherence of the initial system state. It reveals a noteworthy fact that the minimum costs of preparation and measurement are not independent in the WVA scenario. Moreover, they are bounded by the quantum coherence of the system. The theoretical and experimental results agree well and show that increased quantum coherence can reduce the preparation cost and measurement cost jointly. For the initial state with the imperfect coherence resource, we give the optimal strategy to complete the parameter estimation task with the different consumptions of preparation and measurement. We hope that this work will provide some useful assistance in the design of various sensors. Furthermore, our work can be used to explain the advantage of coherent sources in optical super-resolution [27–29], where the coherence can help to reduce the measurement costs.

This work was supported by the National Natural Science Foundation of China (11935012, 12175052, 11775065, 12205092 and 12175075).

* liujingphys@hust.edu.cn

† sunzhe@hznu.edu.cn

‡ xgwang1208@zju.edu.cn

- [1] C. Helstrom, Minimum mean-squared error of estimates in quantum statistics, *Phys. Lett. A* **25**, 101 (1967).
- [2] C. Helstrom, The minimum variance of estimates in quantum signal detection, *IEEE Trans. Inform. Theory* **14**, 234 (1968).
- [3] A. S. Holevo, *Probabilistic and Statistical Aspects of Quantum Theory* (North-Holland, Amsterdam, 1982).
- [4] J. Liu, H. Yuan, X. M. Lu and X. Wang, Quantum Fisher information matrix and multiparameter estimation, *J. Phys. A: Math. Theor.* **53**, 023001 (2020).
- [5] J. R. Janesick et al., *Scientific Charge-Coupled Devices* (SPIE Press, Bellingham, 2001).
- [6] X. M. Lu, X. Wang and C. P. Sun, Quantum Fisher information flow and non-Markovian processes of open systems, *Phys. Rev. A* **82**, 042103 (2010).
- [7] J. Liu, M. Zhang, H. Chen, L. Wang and H. Yuan, Optimal Scheme for Quantum Metrology, *Adv. Quantum Technol.* **5**, 210080 (2022).
- [8] Z. Hou, J. F. Tang, H. Z. Chen, H. D. Yuan, G. Y. Xiang, C. F. Li and G. C. Guo, Zero-trade-off multiparameter quantum estimation via simultaneously saturating multiple Heisenberg uncertainty relations, *Sci. Adv.* **7**, eabd2986 (2021).
- [9] X. M. Lu and X. Wang, Incorporating Heisenberg's Uncertainty Principle into Quantum Multiparameter Estimation, *Phys. Rev. Lett.* **126**, 120503 (2021).
- [10] Y. Aharonov, D. Z. Albert and L. Vaidman, How the result of a measurement of a component of the spin of a spin-1/2 particle can turn out to be 100, *Phys. Rev. Lett.* **60**, 1351 (1988).
- [11] J. Harris, R. W. Boyd and J. S. Lundeen, Weak Value

- Amplification Can Outperform Conventional Measurement in the Presence of Detector Saturation, *Phys. Rev. Lett.* **118**, 070802 (2017).
- [12] S. S. Pang and T. A. Brun, Improving the Precision of Weak Measurements by Postselection Measurement, *Phys. Rev. Lett.* **115**, 120401 (2015).
- [13] S. Pang, J. R. G. Alonso, T. A. Brun and A. N. Jordan, Protecting weak measurements against systematic errors, *Phys. Rev. A* **94**, 012329 (2016).
- [14] A. Nishizawa, K. Nakamura and M. K. Fujimoto, Weak-value amplification in a shot-noise-limited interferometer, *Phys. Rev. A* **85**, 062108 (2012).
- [15] O. Hosten and P. Kwiat, Observation of the Spin Hall Effect of Light via Weak Measurements, *Science* **319**, 787 (2008).
- [16] D. J. Starling, P. B. Dixon, N. S. Williams, A. N. Jordan and J. C. Howell, Continuous phase amplification with a Sagnac interferometer, *Phys. Rev. A* **82**, 011802(R) (2010).
- [17] X. Y. Xu, Y. Kedem, K. Sun, L. Vaidman, C. F. Li and G. C. Guo, Phase Estimation with Weak Measurement Using a White Light Source, *Phys. Rev. Lett.* **111**, 033604 (2013).
- [18] D. J. Starling, P. B. Dixon, A. N. Jordan and J. C. Howell, Precision frequency measurements with interferometric weak values, *Phys. Rev. A* **82**, 063822 (2010).
- [19] P. B. Dixon, D. J. Starling, A. N. Jordan and J. C. Howell, Ultrasensitive Beam Deflection Measurement via Interferometric Weak Value Amplification, *Phys. Rev. Lett.* **102**, 173601 (2009).
- [20] G. Viza, J. Martínez-Rincón, G. A. Howland, H. Frostig, I. Shomroni, B. Dayan, and J. C. Howell, Weak-values technique for velocity measurements, *Opt. Lett.* **38**, 2949-2952 (2013).
- [21] A. N. Jordan, J. Martínez-Rincón and J. C. Howell, Technical Advantages for Weak-Value Amplification: When Less Is More, *Phys. Rev. X* **4**, 011031 (2014).
- [22] G. Bié Alves, B. M. Escher, R. L. de Matos Filho, N. Zagury and L. Davidovich, Weak-value amplification as an optimal metrological protocol, *Phys. Rev. A* **91**, 062107 (2015).
- [23] D. R. M. Arvidsson-Shukur, N. Y. Halpern, H. V. Lepage, A. A. Lasek, C. H. W. Barnes and S. Lloyd, Quantum advantage in postselected metrology, *Nat. Communications* **11**, 3775 (2020).
- [24] A. Feizpour, X. X. Xing and A. M. Steinberg, Amplifying Single-Photon Nonlinearity Using Weak Measurements, *Phys. Rev. Lett.* **107**, 133603 (2011).
- [25] L. J. Zhang, A. Datta and I. A. Walmsley, Precision Metrology Using Weak Measurements, *Phys. Rev. Lett.* **114**, 210801 (2015).
- [26] L. Xu, Z. X. Liu, A. Datta, G. C. Knee, J. S. Lundeen, Y. Q. Lu and L. J. Zhang, Approaching Quantum-Limited Metrology with Imperfect Detectors by Using Weak-Value Amplification, *Phys. Rev. Lett.* **125**, 080501 (2020).
- [27] M. Tsang, R. Nair and X. M. Lu, Quantum theory of superresolution for two incoherent optical point sources, *Phys. Rev. X* **6**, 031033 (2016).
- [28] W. Larson and B. E. A. Saleh, Resurgence of Rayleigh's curse in the presence of partial coherence: comment, *Optica* **5**, 1382–1389 (2018).
- [29] Z. Hradil, J. Řeháček, L. S. Soto and B. G. Englert, Quantum Fisher information with coherence, *Optica* **6**, 1437-1400 (2019).

Appendix A: appendix

For an initial state in the spectral decomposition form $\rho_{in} = \sum_{i=1}^M \lambda_i |\psi_{in,i}\rangle \langle \psi_{in,i}|$, the QIF in the final state $U(g)\rho_{in}U^\dagger(g)$ is

$$F(g) = \sum_{i=1}^M \frac{(\partial_g \lambda_i)^2}{\lambda_i} + \sum_{i=1}^M 4\lambda_i \langle \psi_{in,i} | (\partial_g U^\dagger) (\partial_g U) | \psi_{in,i} \rangle - \sum_{i,j=1}^M \frac{8\lambda_i \lambda_j}{\lambda_i + \lambda_j} |\langle \psi_{in,i} | U^\dagger \partial_g U | \psi_{in,i} \rangle|^2. \quad (\text{A1})$$

Now, we calculate F and F_m for the initial state $\rho_{si} \otimes |\phi_{mi}\rangle \langle \phi_{mi}| = (\mu|\tilde{0}\rangle \langle \tilde{0}| + (1-\mu)|\tilde{1}\rangle \langle \tilde{1}|) \otimes |\phi_{mi}\rangle \langle \phi_{mi}|$. After the unitary evolution $U(g) = \exp(-ig\sigma \otimes M)$, we have

$$\rho_{sm}(g) = U(g) [\rho_{si} \otimes |\phi_{mi}\rangle \langle \phi_{mi}|] U^\dagger(g). \quad (\text{A2})$$

Since $\langle \phi_{mi} | M | \phi_{mi} \rangle = 0$, we have

$$\langle \tilde{x} | \langle \phi_{mi} | U^\dagger \partial_g U | \tilde{y} \rangle | \phi_{mi} \rangle = i \langle \tilde{x} | \sigma | \tilde{y} \rangle \langle \phi_{mi} | M | \phi_{mi} \rangle = 0 \quad (\text{A3})$$

where $\tilde{x} = \tilde{0}, \tilde{1}$; $\tilde{y} = \tilde{0}, \tilde{1}$. At last, we can get

$$F(\rho_{sm}(g)) = 4(\mu \langle \tilde{0} | \sigma^2 | \tilde{0} \rangle + (1-\mu) \langle \tilde{1} | \sigma^2 | \tilde{1} \rangle) \langle \phi_{mi} | M^2 | \phi_{mi} \rangle \quad (\text{A4}) \\ = 4\Omega.$$

With an auxiliary system a , the initial state can be written as $(\sqrt{\mu}|\tilde{0}\rangle|0_a\rangle + \sqrt{1-\mu}|\tilde{1}\rangle|1_a\rangle) |\phi_{mi}\rangle$. After the unitary evolution and postselection, the collapsed state of the meter and the auxiliary system is

$$|\Psi_{am}(g)\rangle = \xi |0_a\rangle (e^{igM} |\phi_{mi}\rangle) + \eta |1_a\rangle (e^{-igM} |\phi_{mi}\rangle) \quad (\text{A5})$$

where $\xi = \frac{\langle \psi_{sf} | \tilde{0} \rangle}{\sqrt{u |\langle \psi_{sf} | \tilde{0} \rangle|^2}}$ and $\eta = \frac{\langle \psi_{sf} | \tilde{1} \rangle}{\sqrt{(1-u) |\langle \psi_{sf} | \tilde{1} \rangle|^2}}$. We can easily get $F(|\Psi_{am}(g)\rangle) = 4\Omega$. Thus, after tracing the auxiliary system, the QIF in the meter can not exceed 4Ω .